Chromosome Research **9**: 569–584, 2001.

Arrangements of macro- and microchromosomes in chicken cells

Felix A. Habermann[1,3], Marion Cremer[1], Joachim Walter[1], Gregor Kreth[2], Johann von Hase[2], Karin Bauer[1], Johannes Wienberg[1], Christoph Cremer[2], Thomas Cremer[1] & Irina Solovei[1]*
[1]*Institute of Anthropology and Human Genetics, University of Munich (LMU), Munich, Germany; Tel: (+49) 89 2180 6713; Fax: (+49) 89 2180 6719; E-mail: irina.solovei@lrz.uni-muenchen.de;* [2]*Kirchhoff-Institute of Physics, University of Heidelberg, Heidelberg, Germany;* [3]*Present address: Chair of Animal Breeding, Technical University of Munich, Freising-Weihenstephan, Germany*
**Correspondence*

Received 21 May 2001; received in revised form and accepted for publication by Herbert Macgregor 5 July 2001

Key words: chicken interphase nuclei, chromosome arrangement, 3D M-FISH, nuclear architecture

Abstract

Arrangements of chromosome territories in nuclei of chicken fibroblasts and neurons were analysed employing multicolour chromosome painting, laser confocal scanning microscopy and three-dimensional (3D) reconstruction. The chicken karyotype consists of 9 pairs of macrochromosomes and 30 pairs of microchromosomes. Although the latter represent only 23% of the chicken genome they contain almost 50% of its genes. We show that territories of microchromosomes in fibroblasts and neurons were clustered within the centre of the nucleus, while territories of the macrochromosomes were preferentially located towards the nuclear periphery. In contrast to these highly consistent radial arrangements, the relative arrangements of macrochromosome territories with respect to each other (side-by-side arrangements) were variable. A stringent radial arrangement of macro- and microchromosomes was found in mitotic cells. Replication labelling studies revealed a pattern of DNA replication similar to mammalian cell nuclei: gene dense, early replicating chromatin mostly represented by microchromosomes, was located within the nuclear interior, surrounded by a rim of late replicating chromatin. These results support the evolutionary conservation of several features of higher-order chromatin organization between mammals and birds despite the differences in their karyotypes.

Introduction

The genomes of all presently existing vertebrate species have diverged from a common ancestor over a period of several hundred million years. The comparative analysis of the genome organization between remote species is a key tool for the delineation of evolutionary conserved features of this organization. While numerous studies have been carried out with regard to the evolutionary changes of genes and karyotypes in mammals (O'Brien *et al.* 1999), data that allow a comparison of nuclear architecture between distant vertebrate species have been lacking so far. The divergence of birds and mammals from a common ancestor occurred about 300—350 million years ago

(Hedges *et al.* 1996). The degree of conserved homologous chromosomal segments between humans and chicken revealed by genetic and physical mapping data is surprisingly high (Burt *et al.* 1999) while the karyotypes are strikingly different. The human genome consists of 2n = 46 chromosomes ranging from 279 Mb to 45 Mb (Lander *et al.* 2001) while the chicken, *Gallus gallus domesticus*, has 2n = 78 chromosomes with a size range between 250 Mb (Smith & Burt 1998) and 3.5 Mb (Pichugin *et al.* 2001). The chicken chromosomes are classified somewhat arbitrarily into two major groups: the macrochromosomes comprise chromosome 1–8 and the sex chromosomes (ZZ, male or ZW, female) with a size ranging from 250 Mb to 30 Mb. The remaining smaller chromosomes are called microchromosomes and cannot be distinguished by conventional banding techniques. Microchromosomes represent approximately 23% of the female genome, are CG-rich and contain about 48% of all genes that have a high content of CpG islands (McQueen *et al.* 1996, 1998, Smith & Burt 1998, Smith *et al.* 2000). On average, microchromosomes appear to have a 2–4 times higher gene density than the macrochromosomes (Smith *et al.* 2000). The macrochromosomes are AT-rich and exhibit weak R-, C-, and T-banding (Schmid *et al.* 1989). The chicken genome (about 1200 Mb, Smith *et al.* 2000) is distinctly smaller than the human genome (3300 Mb, Lander *et al.* 2001). The smaller genome size in birds is mainly due to a lower content of repetitive sequences (Primmer *et al.* 1997).

The availability of specific DNA probes that delineate entire individual chromosomes and chromosomal subregions down to the level of individual gene loci has made possible detailed studies of chromosome structure and their arrangement in the nuclei of human cells. Recently, specific chromosome paint probes have also become available for all chicken macrochromosomes, several of the larger microchromosomes, and for fractions of smaller microchromosomes (Griffin *et al.* 1999). The availability of this probe set has prompted us to study chromosome territory arrangements in chicken cell nuclei for comparison with the data known for human cells. The following questions were posed: (1) Can we confirm a territorial organization of chromosomes in chicken cell nuclei? (2) Are neighbourhoods (side-by-side arrangements) of chicken chromosome territories fixed or variable as noted for several human cell types (see Cremer *et al.* 2001)? (3) Do chicken nuclei exhibit specific radial arrangements of chromosome territories depending on different parameters such as chromosome size, gene density and replication timing as observed in humans and other mammalian species (see Cremer *et al.* 2001)? We performed multi-colour FISH on three-dimensionally (3D) preserved nuclei of embryonic chicken fibroblasts and neurons. In addition, replication labelling with halogenated thymidine analogues was employed to study the nuclear distribution of early and mid-to-late replicating chromatin.

Materials and methods

Cell culture

Embryonic chicken fibroblasts were isolated from 5–6-day-old chicken embryos and grown at 39°C and 3% CO_2 in Dulbecco's minimal essential medium (DMEM) containing 4.5 mg/ml glucose and 2 mmol/L L-glutamine, supplemented with 10% fetal calf serum (FCS) and 100 U/ml penicillin/100 μg/ml streptomycin. Primary neuronal cell cultures were prepared from the telencephalon of 7-day-old chicken embryos as described by Pettmann *et al.* 1979. Cerebral hemispheres were mechanically dissociated by passing through a nylon mesh (mesh size 48 μm). The resulting cell suspension was seeded at an approximate cell density of 4×10^4 cells/cm^2 on poly-L-lysine (MW 70–100 kDa, Sigma, Germany) coated coverslips and cultured in 80% DMEM and 20% fetal calf serum for 6 days. Medium was changed every 24 h. The outgrowth of neurites started 12 hours after seeding, building up a branched network during the time of cultivation. Chicken lymphoblastoid cell line DT-40 was kindly provided by Dr. J.-M. Buerstedde (Heinrich-Pette Institute for Experimental Virology and Immunology, University of Hamburg) and was grown in RPMI 1640 supplemented with 10% FCS and 2% chicken serum.

Generation of labelled pools of chromosome-specific painting probes

For multicolour FISH, we prepared pools containing several chromosome-specific painting probes. These probes were obtained from flow-sorted chicken chromosomes (Griffin *et al.* 1999) and amplified by DOP-PCR using the 6MW primer (Telenius *et al.* 1992). Probe pools were re-amplified by stringent DOP-PCR and subsequently labelled with biotin- or digoxigenin-dUTP (Roche, Germany) by DOP-PCR or with estradiol-dUTP (Roche, Germany) using a standard nick-translation protocol. Two sets of probe pools were prepared: (I) Probe pools for differential painting of the macrochromosomes 1–6 and Z by combinatorial labelling. Pool Ia, including chromosomes 1, 4, 5 and 6, was labelled with biotin-dUTP; pool Ib, including chromosomes 2, 4, 6 and Z, was labelled with digoxigenin-dUTP; pool Ic, including chromosomes 3, 5, 6 and Z, was labelled with estradiol-dUTP. (II) To study the size-correlated distribution of chromosome territories, three other probe pools were prepared. Pool IIa, detecting the macrochromosomes 1–5 and Z, was labelled with biotin-dUTP; pool IIb, detecting the medium-sized chromosomes 6–10, was labelled with estradiol-dUTP; pool IIc, detecting 19 microchromosomes, was labelled with digoxigenin-dUTP. The pool of medium-sized chromosomes 6–10 takes into account that chromosome 6 is notably smaller than chromosome 5 and that chromosome 10 is notably larger than the remaining microchromosomes (see Figures 1C, 2B).

Fluorescence in-situ *hybridization on metaphase spreads (2D FISH)*

The labelled probe pools were mixed with a 10-fold excess of chicken Cot-1 DNA, ethanol-precipitated and resuspended in 50% deionised formamide, 10% dextran sulphate and $1 \times$ SSC to a final concentration of 20–40 ng/μl for each single probe. Probes were denatured at 75°C for 5 min and allowed to pre-anneal for 20 min at 37°C before hybridization. Metaphase spreads from fibroblasts and DT-40 cells were prepared following standard protocols. Slides with metaphase spreads were denatured in 70% formamide/$2 \times$ SSC, pH 7.0 at 70°C for 2 min, dehydrated in an ethanol series and air-dried before probe loading. Hybridization was performed at 37°C for 72 h. Post-hybridization washes included $2 \times$ SSC at 37°C and $0.1 \times$ SSC at 60°C. Biotin was detected by Avidin-Cy3 (Dianova, Germany), digoxigenin by a monoclonal mouse anti-digoxigenin antibody (Roche, Germany) and a FITC-conjugated sheep anti-mouse antibody. Oestradiol was detected by an anti-oestradiol antiserum from rabbit (Roche) and a Cy5-conjugated goat-anti-rabbit antibody (Dianova, Germany). Chromosomes were counterstained with DAPI and mounted in Vectashield (Vector Laboratories, UK).

FISH on three-dimensionally preserved nuclei (3D-FISH)

A detailed protocol for 3D-FISH employed in our laboratory is described elsewhere (Solovei *et al.* 2001). Cells were seeded on coverslips (thickness 0.170 ± 0.01 mm) in quadruple cell culture chambers (Quadriperm, Heraeus, Germany) and cultured for 72 h (fibroblasts) or 6 days (neurons). Cells were fixed under isotonic conditions in 1.3% paraformaldehyde in $0.5 \times$ PBS for 15 min at RT. Permeabilization steps included: (1) treatment with 0.5% Triton X100 for 20 min, (2) incubation in 20% glycerol in PBS for 30 min, (3) repeated freezing in liquid nitrogen and thawing at RT, and (4) incubation in 0.1 N HCl for 5 min. Coverslips with cells were kept in 50% formamide/$2 \times$ SSC at 4°C until hybridization. Hybridization conditions, post-hybridization washings and detection procedures were essentially the same as described for 2D FISH on metaphase chromosomes with the exception that cells were strictly prevented from drying. Therefore, after denaturation of cells in 70% formamide/$2 \times$ SSC, pH 7.0 at 72°C for 2 min, they were immediately quenched in ice-cold 50% formamide/$2 \times$ SSC before probe loading.

Replication labelling of DT-40 cells and fibroblasts

For replication banding of chicken metaphase chromosomes, asynchronously growing DT-40 cells were incubated for 1 h with the thymidine

analogue iododeoxyuridine (IdU, Sigma, final concentration 1 μmol/L). Cells were washed twice with PBS and further incubated in RPMI medium. Six hours after the end of the first label, cells were exposed to chlorodeoxyuridine (CldU, Sigma, final concentration 1 μmol/L) for 1 h, and washed twice again with PBS. After further growth in label-free RPMI medium for 4 h, metaphase spreads were prepared following standard protocols. The same labelling protocol was employed for the delineation of early and late replicating chromatin in 3D-preserved nuclei of proliferating chicken fibroblasts with the modification that the interval between the two labels was 5 h and cells were fixed immediately after the second pulse. For detection of IdU and CldU, the DNA of metaphase chromosomes and 3D-preserved fibroblast nuclei was denatured in 70% formamide at 72°C as described above. Incorporated IdU was detected using mouse-anti-BrdU (Clone B44, Becton Dickinson, UK) and Alexa 488-conjugated goat anti-mouse antibody (Molecular Probes, NL); CldU was detected using a monoclonal rat-anti-CldU antibody (Clone Bu/75, Oxford Biotechnology, UK) and Cy3-conjugated goat-anti-rat antibody (Amersham, UK). IdU and CldU were detected sequentially to avoid antibody cross-reactions (for a detailed description, see Solovei *et al.* 2001).

Microscopy

Metaphase spreads were analysed using an epifluorescence microscope (Axioplan II, Zeiss, Germany) equipped with a PlanApochromat $100\times/1.4$ oil immersion objective and filter sets for DAPI, FITC, Cy3 and Cy5. Digital images were acquired by a CCD-camera (CoolView, Photonic Science, UK) using CytoVision software (Applied Imaging, UK). The 8-bit greyscale single channel images were overlaid to a RGB image, assigning a false colour to each channel. Light optical serial sections of cell nuclei were recorded by a confocal microscope (LSM 410, Zeiss) equipped with a PlanApochromat $63\times/1.4$ oil-immersion objective, three laser channels (excitation lines 488 nm, 543 nm, 633 nm), and the following emission filters: 510–525-nm bandpass for FITC, 575–640 nm bandpass for Cy3, and 665-nm longpass for Cy5. For each focus plane, the three fluorochromes were recorded sequentially generating 8-bit greyscale images. Pixel size was 50×50 nm; the axial distance between optical sections was 250 nm. To obtain an improved signal-to-noise ratio, each section image was averaged from 32 successive scans.

Digital image processing

The confocal image stacks were corrected for chromatic shift and subjected to deconvolution using the software Huygens 2 (Scientific Volume Imaging b.v., Hilversum, NL), running on a silicon graphics O2 workstation, OS IRIX 6.5. For deconvolution a theoretical point spread function was applied, considering the pixel size, the distance between the optical sections, the numerical aperture of the objective, pinhole size, refractive indices of mounting medium and immersion oil as well as the signal-to-noise ratio. The deconvolved image stacks were used to generate 3D reconstructions of chromosome territories by surface rendering using 3D image software Imaris (version 2.7, Bitplane AG, Switzerland). Chromosome assignment for combinatorially labelled chromosomes was done by visual inspection of the resulting pure or mixed colours.

Quantitative analysis of the size-correlated distribution of chromosome territories

For a quantitative evaluation of the chromatin distribution from the three chromosome sets for large, medium-sized, and microchromosomes (described as probe pools IIa–c in Methods), a central optical section from each nucleus was analysed (for detailed description see Cremer *et al.* 2001).

Simulation of the chromosome territory arrangement in ellipsoid cell nuclei

To obtain a statistical distribution of chromosome territories that would be expected as a consequence of geometrical constraints, computer simulations were performed using the "spherical 1-Mbp chromatin domain (SCD) model" (for details, see Cremer *et al.* 2000, Cremer & Cremer 2001, Kreth *et al.* 2001). The simulation experiments assumed an ellipsoid nuclear shape with

half axes of 4:2:2 μm and took into account the approximate size of chicken chromosomes according to Smith & Burt 1998. Chicken chromosomes were divided into three groups: (1) the macrochromosomes 1–4 and Z, (2) the medium-sized chromosomes 5–8 and W, (3) a set of 19 microchromosome pairs ranging in size from 14 Mb down to 4 Mb. Each group of chromosome territories was visualized in a separate colour by applying virtual microscopy techniques (Cremer *et al.* 2001). For a quantitative evaluation, a central section from each nucleus was analysed in exactly the same way as described for light optical sections of painted chicken nuclei.

Results

Variable side-by-side arrangements and structural features of macrochromosome territories 1–6 and Z

For differential painting of the 6 largest autosomes and the Z-chromosome by multi-colour FISH, a combinatorial labelling scheme was established as shown in Figure 1A. For this purpose, the labelled probe pools were first tested individually and in combination on metaphase spreads. The concentration of individual chromosome-specific paint probes within each pool was adjusted to achieve a strong and rather homogeneous signal intensity on each painted chromosome. These adjusted pools were mixed and hybridised to metaphase spreads. Each chromosome could be identified visually based on its distinct fluorescence pattern (Figure 1B). The same probe pools were hybridised to 3D-preserved nuclei of fibroblasts and neurons. Observations of different optical sections demonstrated that each macrochromosome occupied a distinct territory (Figure 1D, E, G, H, I) with clear boundaries between adjacent territories. Deconvolution of the image stacks showed that the territories were built up of chromatin domains that have the appearance of granules (Figure 1E, H) with diameters of 300–600 nm. Chromatin domains of similar size and morphology were also found in optical sections of chicken fibroblast nuclei stained with propidium iodide (data not shown), as well as in nuclei labelled with halogenated thymidine analogues (Figure 4C).

The spatial arrangement of differentially painted macrochromosomes in chicken nuclei was studied using confocal serial sections from 20 fibroblasts and 20 neurons. The side-by-side arrangement of the macrochromosome territories, e.g. the relative arrangement of chromosome territories with respect to each other, varied from cell to cell (compare, e.g. Figure 1E, H and I). The territories of homologous chromosomes were found to be separate in most instances, although homologous associations were also observed (see Figure 1H, chromosome 1 and 4 territories). Sister nuclei in binucleated fibroblasts showed strikingly similar – either congruent or mirror-like symmetrical – arrangements of macrochromosome territories. (Figure 1I and J). However, the comparison of different pairs of sister nuclei confirmed the high intercellular variability of side-by-side chromosome territory arrangements observed in mononucleated fibroblasts and neurons (data not shown).

Distinct radial arrangements of macro- and microchromosome territories

To study the question of whether the radial position of chromosome territories within the nucleus is correlated with their DNA content, chicken chromosomes were assigned to three categories according to their size. Each category was stained with a separate fluorochrome by preparing three chromosome paint pools: Pool IIa labelled the macrochromosomes 1–5 and Z, pool IIb labelled the medium-sized chromosomes 6–10 (e.g. the macrochromosomes 6–8 and the two largest microchromosome pairs) and pool IIc labelled 19 microchromosome pairs (Figure 1C, 2B). The chromosomes painted by these three probe pools account for about 95% of the chicken genome (according to Smith & Burt 1998). Three-colour FISH on metaphase spreads demonstrated strong signals for each pool without cross-hybridization (Figure 2A). The same three probe pools were hybridised to three-dimensionally preserved nuclei from neurons and fibroblasts. While the cultured neurons did not show any proliferative activity, about 10% of the fibroblasts were in S-phase as revealed by BrdU pulse labelling (data not shown). A series of confocal sections through a neuron nucleus is

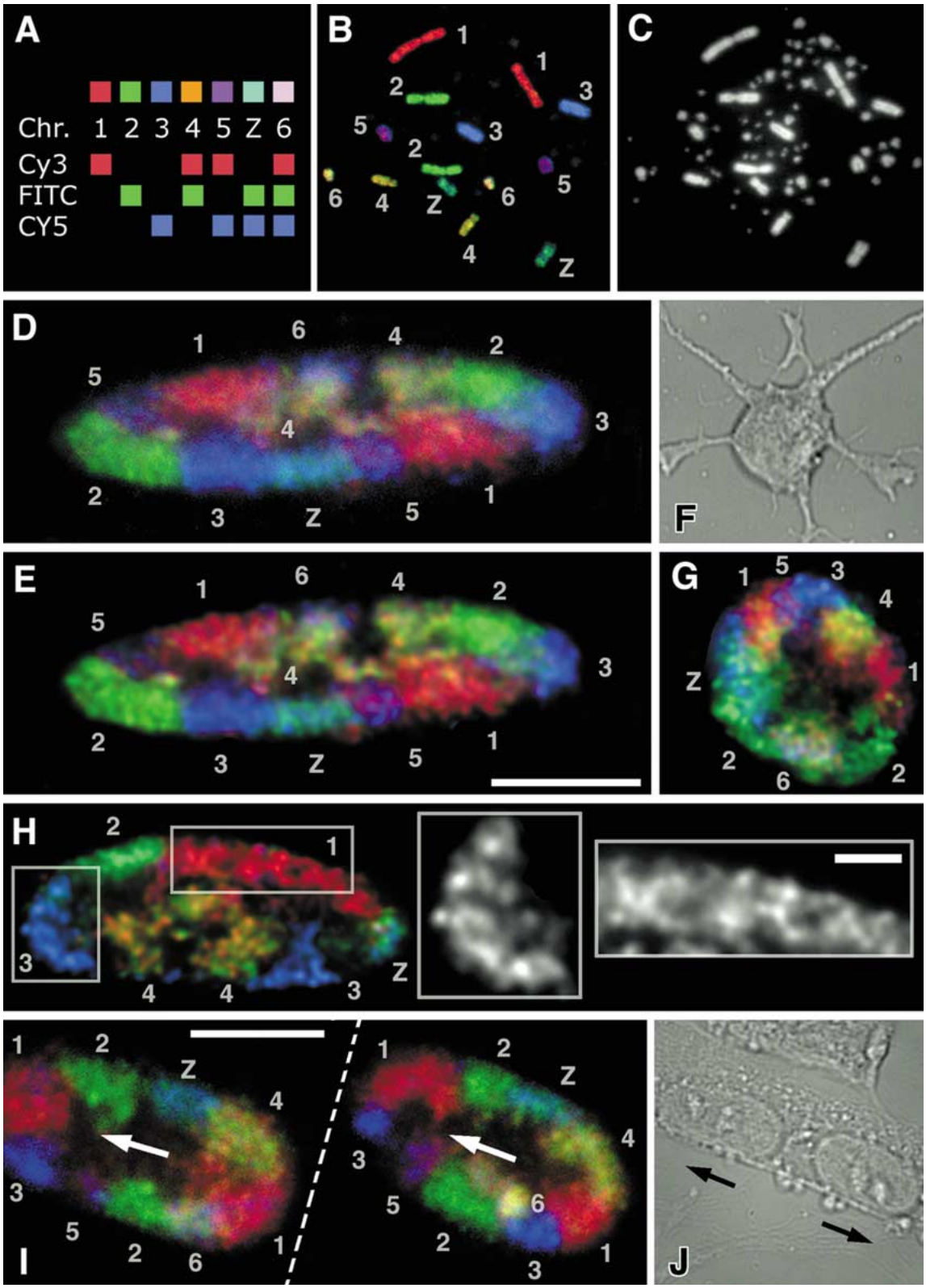
A
Chr. 1 2 3 4 5 Z 6
Cy3
FITC
CY5
B
C
D
F
E
G
H
I
J

shown in Figure 2C, a central section through a fibroblast nucleus is shown in Figure 2F. The image stacks were used to compute 3D reconstructions that can be rotated and viewed from different sides (Figure 2E, G). The visualization of the three chromosome pools revealed a consistent radial arrangement pattern. In both, fibroblast and neuronal cells, the sets of large chromosomes (1–5, Z) and medium-sized chromosomes (6–10) were found predominantly at the periphery of the nucleus, while the set of 19 microchromosome pairs formed clusters predominantly located in the inner part of the nucleus. However, some microchromosomes reached the surface of the nucleus forming small microchromosomal patches between macrochromosomes (Figure 2 C, E, F and G).

The distribution of the three chromosome sets was quantitatively analysed in 21 neuron nuclei and 28 fibroblast nuclei evaluating a central optical section of each nucleus. The resulting graphs are shown in Figure 3. Fibroblast nuclei showed an almost identical distribution for the macro- and the medium-sized chromosome territories with a maximum DNA content at approximately 80% of the relative radius. In neurons, the distribution of the macrochromosomes 1–5 and Z showed a maximum DNA content at 78% of the relative radius, while the distribution of the medium-sized chromosome territories was shifted slightly towards the interior with a maximum DNA content at 73% of the relative radius. In comparison with the larger chromosome territories, in both cell types, the territories of the microchromosome set were clearly shifted towards the centre of the nuclear section with a peak of the DNA content at 62% in neurons and at 55% in fibroblasts. In neurons, the centre of the nucleus was typically occupied by one large nucleolus (Figure 2C, optical section #4), while the positions of nucleoli (1–2 per nucleus) in fibroblasts varied. Accordingly, in neuron nuclei, the peak of the distribution curve for the microchromosome pool was shifted somewhat more to the periphery than in fibroblasts.

Three-dimensional simulation of statistically distributed large, medium-sized and small chromosome territories in ellipsoid cell nuclei

To compare the observed radial distribution of large, medium-sized and small chromosome territories with a statistical distribution resulting from geometrical constraints, the distribution of the three chromosome groups was simulated in 50 ellipsoid model cell nuclei and quantitatively analysed evaluating a virtual central section of each model nucleus. An example of such a nucleus and a virtual microscopic section are shown in Figures 2H and 2I. The results of these computer simulations were opposite to the results of the FISH experiments: the large territories were predominantly located in the nuclear centre with a peak of maximum DNA content at 55%, while the smaller chromosome territories were predomi-

Figure 1. (*opposite*) Simultaneous visualization of chicken macrochromosomes 1–6 and Z by multicolour FISH (M-FISH) on metaphase spreads and 3D preserved cell nuclei. (**A**) Scheme of combinatorial labelling for 7-colour FISH experiments (for details see Methods). (**B**) Chicken (ZZ) metaphase spread after 7-colour painting. False colours were attributed to the painted chromosomes 1–6 and Z depending on the different combinations of fluorochromes explained in (**A**). (**C**) The same metaphase counterstained with DAPI. (**D**) Mid-plane optical section through a chicken (ZW) fibroblast nucleus with seven pairs of painted chromosomes. All macrochromosomes occupy distinct territories and are arranged along the nuclear periphery. Note that only one of the two chromosome 6 territories is represented in this section. (**E**) After deconvolution of the same section, the granular substructure of the chromosome territories becomes apparent. (**F**) Transmission light image of a chicken neuronal cell showing an axon and several dendrites. (**G**) Central light optical section through the nucleus of the cell shown in (**F**) after 7-colour painting of the macrochromosomes 1–6 and Z and deconvolution. Painted chromosome territories are seen at the nuclear periphery. The unstained area in the centre of the section corresponds to a large nucleolus and space occupied by microchromosomes (compare with Figure 2C). (**H**) Mid-plane confocal section of another fibroblast nucleus after deconvolution. Macrochromosomes represented in this section are also situated at the periphery of the nucleus, but their side-by-side arrangement is different from that in the nucleus shown in (**D**) and (**E**). The granular substructure of chromosome territories 1 and 3 is exemplified at higher magnification (boxes). (**I and J**) Two daughter fibroblast nuclei show a mirror-like symmetrical distribution of macrochromosomes. To facilitate comparison of the chromosome arrangements, the right nucleus in (**J**) was rotated at 180° in (**I**). The bar on (**E**) and (**I**) is 5 μm, the bar on the insertion in (**H**) is 1 μm.

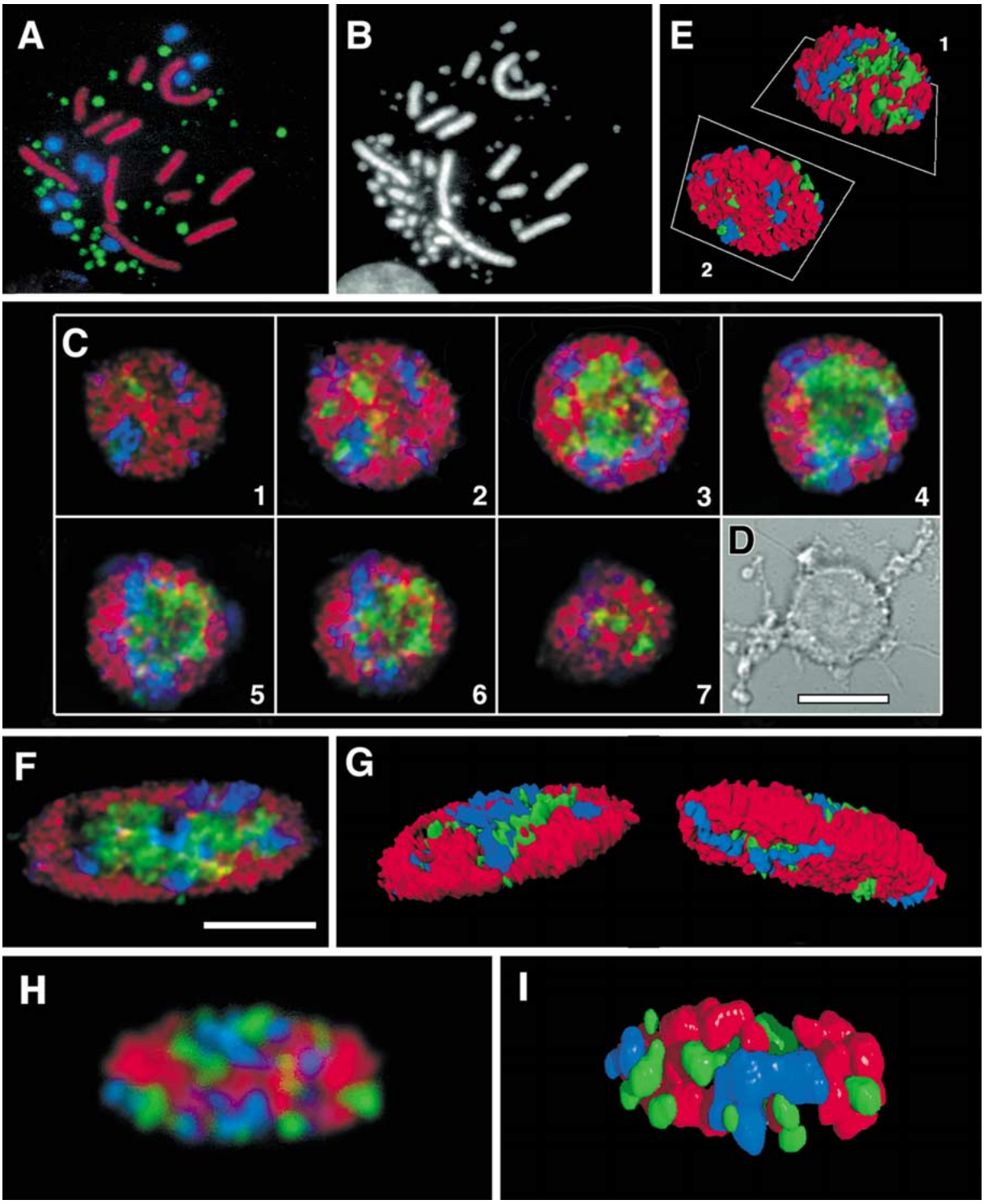
A
B
E
1
2
C
1
2
3
4
5
6
7
D
F
G
H
I

nantly located at the nuclear periphery with a maximum DNA content at around 80% of the nuclear radius (Figure 3).

Distribution of macro- and microchromosomes in mitotic cells

The probe pools for macro- and microchromosomes were also used for the analysis of the radial arrangement of chicken chromosomes in 3D preserved mitotic cells in growing fibroblast cultures. Late prophase and prometaphase rosettes presented a strikingly consistent size-correlated distribution of chromosomes: a central, round or star-shaped cluster of microchromosomes encircled by macrochromosomes (Figure 5A, B). This order was maintained throughout metaphase, anaphase (Figure 5C, D) and telophase.

The distribution of early and late replicating chromatin during S-phase

To define early and late replicating chromatin in metaphase chromosomes from DT-40 cells, double replication labelling experiments with IdU and CldU were performed (for labelling schemes see Materials and methods). In the following, we use the terms ''early'' to assign chromatin replication roughly to the first half of S-phase (i.e. labelled with the first labelling pulse) and ''late'' to the second half of S-phase (i.e. labelled by the second labelling pulse), respectively. This pragmatic definition does not refer to the specific labelling patterns described for different stages of S-phase in mammalian cell nuclei (O'Keefe *et al.* 1992). We showed that chicken microchromosomes predominantly consist of early replicating chromatin, while most of the chromatin of macrochromosomes replicates late (Figure 4A,B). Some microchromosomes also contain late replicating chromatin (Figure 4A,B, arrows). To study the spatial arrangement of early and late replicating chromatin in 3D preserved nuclei of embryonic chicken fibroblasts, asynchronously growing cells were double labelled with IdU and CldU (for description see Materials and methods) and fixed immediately after the second label. As shown in Figure 4C, late replicating chromatin was preferentially located at the periphery of the nucleus, while early replicating chromatin occupied mostly the nuclear interior. Hence, the distribution of early and late replicating chromatin is congruent with the distinct radial position of small and large chicken chromosome territories.

Discussion

Macro- and microchromosome territories show morphological characteristics similar to mammalian chromosome territories

Chromosome territories in interphase nuclei of chicken embryonic fibroblasts and neuronal cells displayed variable shapes and were built up from

Figure 2. (*opposite*) (**A–G**) Visualization of macrochromosomes 1–5 and Z (false coloured in red), medium-sized chromosomes 6–10 (blue) and 19 pairs of microchromosomes (green) on metaphase chromosomes and in 3D preserved cell nuclei by FISH. (**A**) Chromosome painting of a chicken (ZZ) metaphase spread. (**B**) The same metaphase spread after counterstaining with DAPI. Note that most but not all microchromosomes are painted. (**C–E**) Distribution of chromosome territories in the nucleus of a neuron. (**C**) Gallery of deconvolved images from confocal serial sections obtained after 3-colour painting of macrochromosomes, medium-sized chromosomes and microchromosomes. Every second optical section is shown, the distance between sections is 500 nm. Macrochromosomes (red) and medium-sized chromosomes (blue) are situated peripherally, while microchromosomes (green) are located more centrally except for a few clusters that expand towards the nuclear periphery (e.g. optical section #4, 6). The central part of the nucleus on the mid plane sections (#4, 5) is devoid of chromatin due to the centrally located large nucleolus. (**D**) Transmission light image. (**E**) 3D reconstruction by surface rendering: top view (1) and bottom view (2). (**F, G**) Distribution of chromosome territories in the nucleus of a fibroblast. Mid-plane optical section (**F**) and 3D reconstruction (**G**) shown from top (left) and from bottom (right). Note a peripheral localization of macrochromosomes (red) and medium-sized (blue) chromosomes, and central position of most microchromosomes (green). (**H and I**) Computer simulation of large (red), medium-sized (blue) and small (green) chromosome territories in a virtual ellipsoid cell nucleus could not explain the consistent size-correlated radial arrangements of chromosome territories observed in chicken cell nuclei by a statistical distribution influenced by geometrical constraints. (**H**) Virtual microscopic section through the mid plane of a simulated cell nucleus. (**I**) 3D reconstruction of the same nucleus.

focal chromatin domains of a size roughly between 300 and 600 nm. These focal domains are comparable in size to the ~1-Mb chromatin domains previously described in human chromosome territories (Zink *et al.* 1998, Cremer *et al.* 2000, Cremer & Cremer 2001). These ~1-Mb chromatin domains are presently not well defined at the electron microscopic level. They are maintained throughout the cell cycle. During S-phase, they recruit replication factors and represent at this time period replication foci (Leonhardt *et al.* 2000). In mitosis, several adjacent domains form chromosome bands (Sadoni *et al.* 1999).

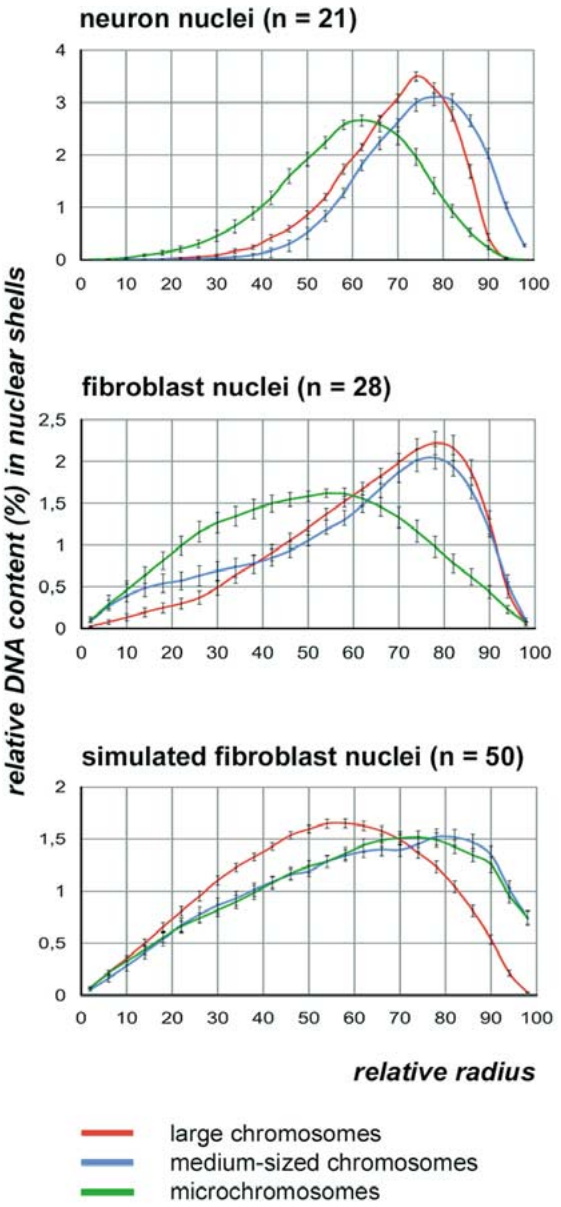

Figure 3. Quantitative evaluation of the DNA-content distribution from large, medium-sized, and microchromosomes on central optical sections through nuclei of chicken neurons and fibroblasts as well as simulated ellipsoid cell nuclei. For a detailed description of the mapping of radial chromosome territory arrangements, see Cremer *et al.* 2001. The abscissa denotes the relative radius *r* of the 25 concentric nuclear areas evaluated in each central section. The ordinate represents the normalized relative DNA content of painted chromosome territories in a given area. For this purpose, all pixel intensities of the fluorochrome employed for chromosome territory painting were summed up within a given area. For normalization, the total relative DNA content for the chromosome territories painted with a given fluorochrome was summed up over all 25 concentric areas and was set to 100. Bars represent standard deviations of the mean. The observed distribution of chromosome territories in fibroblast nuclei is in contrast to a statistical distribution that was obtained by simulating a random arrangement of chromosome territories in ellipsoid cell nuclei with respect to topological constraints.

Side-by-side arrangements of macrochromosome territories are variable

Based on the visual inspection of fibroblast and neuronal nuclei after multicolour painting of the seven largest macrochromosomes, we conclude that neighbourhoods between non-homologous as well as homologous macrochromosome territories are variable. Territories of homologous macrochromosomes were, in most cases, separated even in remote nuclear positions, although associations were also observed. We also could not notice any obvious difference between side-by-side arrangements of chromosome territories and proliferating activity of the cells: in both cycling fibroblasts and non-proliferating neurons, the side-by-side arrangement of macrochromosome territories varied from cell to cell. These findings are in agreement with previous studies of different human cell types demonstrating a pronounced cell-to-cell variability of chromosome territory neighbourhoods (Emmerich *et al.* 1989, Popp *et al.* 1990, Dietzel *et al.* 1995, Lesko *et al.* 1995, Sun & Yokota 1999, Sun *et al.* 2000, Cremer *et al.* 2001). However, based on presently available data, the possibility remains that specific chromo-

some segments have a high probability, even a functional necessity to be placed close to each other in certain cell types, at certain stages of the cell cycle or in terminally differentiated cells.

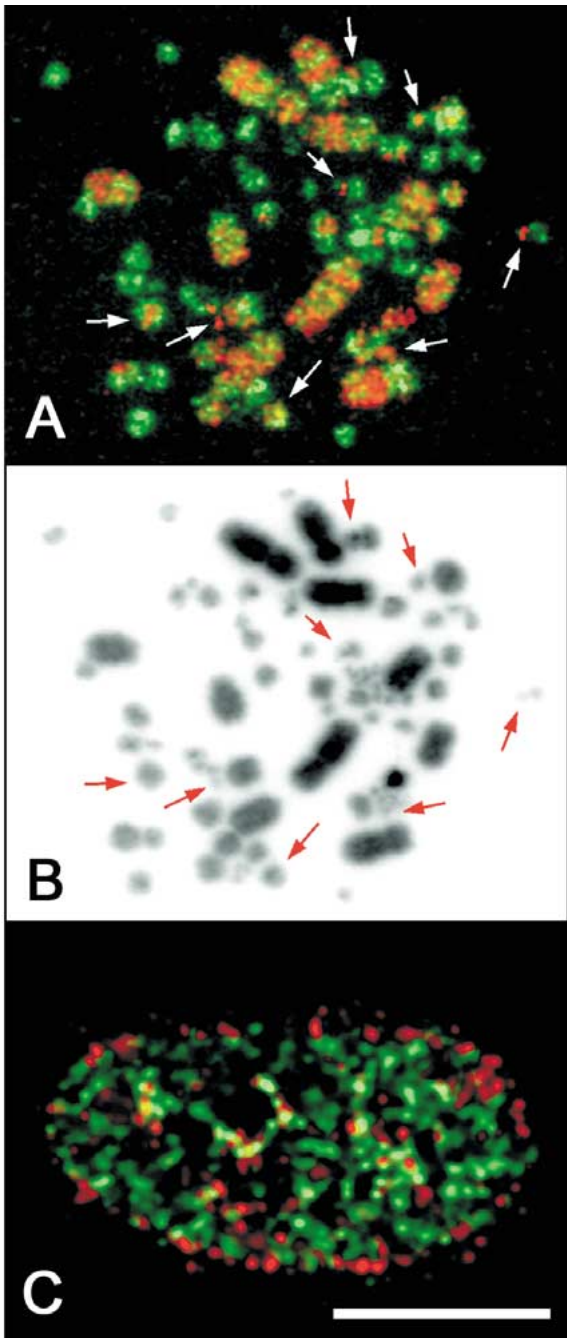

Figure 4. (**A**) Metaphase chromosome spread from a DT-40 cell after double replication labelling. Early replicating chromatin (green) is observed mainly in micro- and medium-sized chromosomes, while macrochromosomes contain mostly later replicating chromatin (red). Arrows show small sites of late replicating chromatin on some microchromosomes. (**B**) Inverted DAPI image of the metaphase spread. Arrows show the same microchromosomes as shown in (**A**). (**C**) Light optical section through the mid part of a double replication labelled primary chicken fibroblast nucleus. Note a rim of late replicating chromatin foci (red) at the nuclear periphery. Early replicating chromatin foci (green) together with some late replicating foci are located in the nuclear interior. Bars = 5 μm.

Radial arrangements of macro- and microchromosomes are highly consistent in interphase nuclei and mitotic figures

In contrast to the pronounced intercellular variability observed for side-by-side arrangements of homologous and non-homologous chromosome territories, the radial arrangements of macro- and microchromosomes were highly consistent. Macrochromosome territories were located mostly towards the nuclear periphery, while microchromosome territories formed a few distinct clusters located towards the nuclear centre. This was observed in proliferating chicken fibroblasts as well in non-proliferating neurons suggesting that this radial arrangement may be a general motif of chicken cell types. In parallel, dividing fibroblasts displayed a stringent radial chromosome arrangement in all stages of mitosis – a central microchromosome cluster surrounded by a ring of macrochromosomes.

Such a size-correlated arrangement of mitotic chromosomes was first noted on squashed preparations of proliferating tissues from different species including chicken (for references see White 1961). In these studies, the preferential location of small chromosomes in the central part and of large chromosomes in the periphery of metaphase plates was described. The squashing technique (Mcgregor & Varley 1988) preserves the *in-vivo* arrangement of mitotic chromosomes to a certain degree. Despite the fact that the commonly used spreading technique employing colcemide and hypotonic treatment is much more destructive, a similar distribution pattern of large and small chromosomes was also observed in metaphase

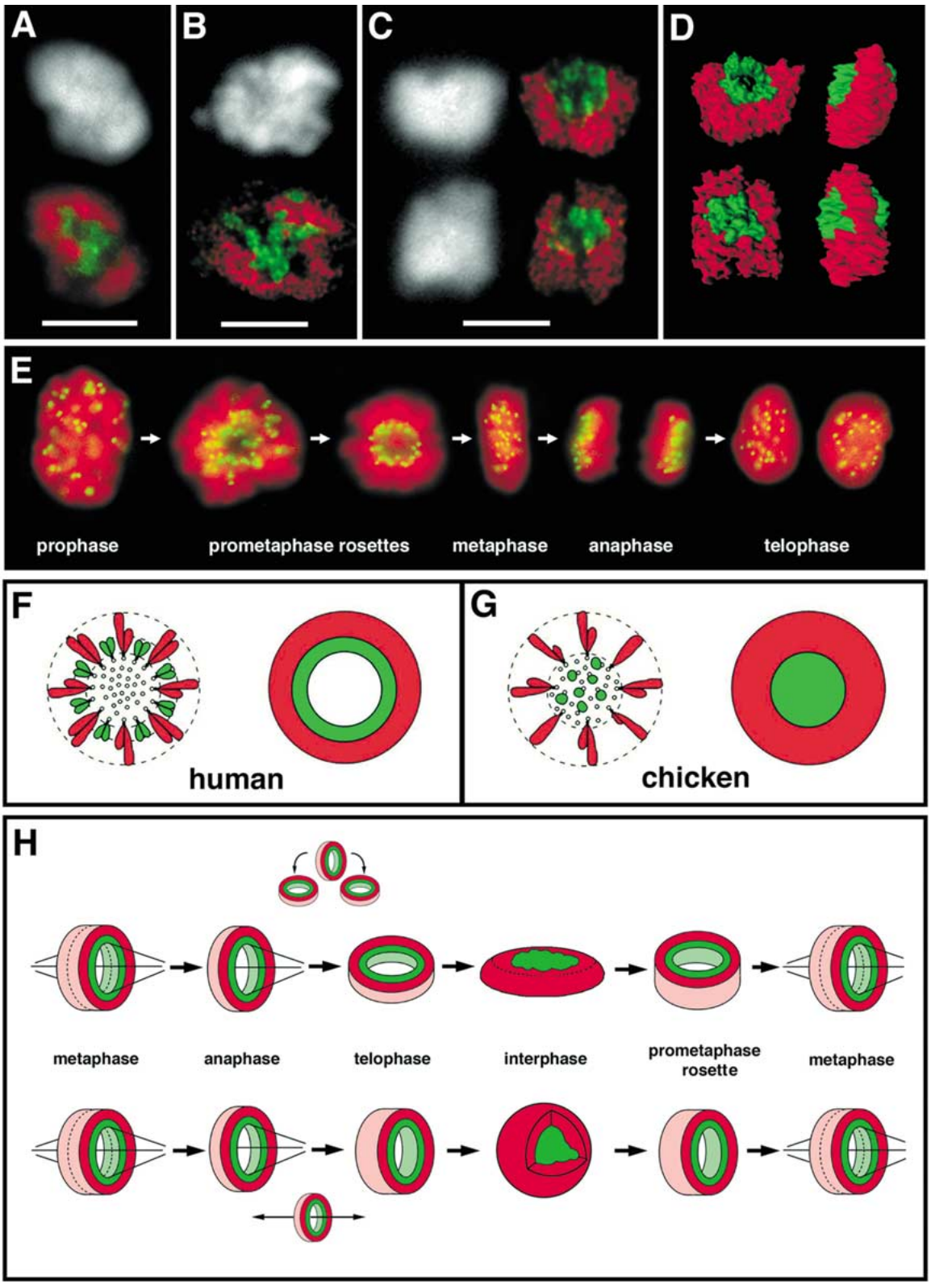
A
B
C
D
E
prophase
prometaphase rosettes
metaphase
anaphase
telophase
F
human
G
chicken
H
metaphase
anaphase
telophase
interphase
prometaphase rosette
metaphase

spreads from human lymphocytes and fibroblasts (for references, see Cremer *et al.* 2001). These findings suggest that chromosome arrangements noted in mitotic cells correlate to some extent with chromosome territory arrangements in interphase nuclei.

The mechanisms that maintain the observed radial arrangements of micro- and macrochromosomes in chicken cells from one cell cycle to the other are not known. Computer simulations of chromosome territories in ellipsoid cell nuclei show that these radial arrangements of macro- and microchromosome territories cannot be explained by a statistical distribution of large and small chromosome territories influenced by topological constraints.

Epigenetic mechanisms, including DNA-methylation and histone acetylation, apparently play a major role in higher-order chromatin architecture and gene expression (Rice & Allis 2001, Wade 2001) but their potential contribution to the intranuclear arrangements of chromosome territories has not been studied so far. Gene-poor mid-to-late replicating chromatin may – in contrast to early replicating gene-dense chromatin – carry binding sites for the reconstituting nuclear lamina during telophase (Pyrpasopoulou *et al.* 1996). This could push early replicating gene-dense chromatin into a more interior position, a finding also observed in mammalian cell nuclei (Sadoni *et al.* 1999, Schermelleh *et al.* 2001 and references therein). However, late-replicating chromatin was also observed around the nucleoli. At present, the system of molecular ''addresses'' that may account for the formation of separate higher order chromatin compartments formed by polarized chromosome territories (Sadoni *et al.* 1999, 2001) is mainly subject to speculations.

To some extent the size-correlated radial arrangement of chromosome territories in interphase cell nuclei may be due to the organization of the mitotic spindle (see Figure 5E–H). The central part of a mitotic spindle in vertebrates consists of a tight bundle of microtubules stretching between the two centrioles. In species with very small chromosomes (like birds), the latter may find enough space between the central microtubules of the spindle, and may therefore be located centrally, while larger chromosomes occupy a ring-shaped zone outside the central bundle of microtubules (Figure 5G; Östergren 1945, White 1961). In human cells, even smaller chromosomes may be large enough to be excluded from the spindle centre and hence to abut the tight bundle of central spindle microtubules (Östergren 1945, Bajer & Molé-Bajer 1972, Chaly & Brown 1988, Rieder & Salmon 1994, Nagele *et al.* 1995).

Figure 5. (*opposite*) Maintenance of the size-correlated distribution of chromosomes through the cell cycle. (**A–D**) Distribution of microchromosomes (green) and macrochromosomes (red) in prophase nuclei (**A**), prometaphase rosettes (**B**), and late anaphase rosettes (**C, D**) from embryonic chicken fibroblasts. Note peripheral position of macrochromosomes and central location of microchromosomes throughout all stages of mitosis. Black-and-white figures show counterstaining with DAPI. A 3D reconstruction (surface rendering) of anaphase rosettes from (**C**) is shown on (**D**): top (left) and lateral (right) views. Bars: 5 μm. (**E**) Arrangement of chromosomes and centromeres through mitosis in adherently growing human cells (primary fibroblasts). Chromosomes were stained with DAPI (red); location of centromeres (green) was defined with antibodies against CENP-C (kind gift from W.C. Earnshaw, University of Edinburgh). At the beginning of the prophase, centromeres are predominantly situated at the nuclear periphery. At the end of the prometaphase, all centromeres become attached to microtubules and form a ring-like structure around the bundle of central microtubules of the mitotic spindle. This ring-like arrangement of centromeres persists during the metaphase and anaphase. At the end of the telophase – beginning of the G1 stage, most of the centromeres return to the periphery of the nucleus. (**F, G**) Scheme illustrating the arrangement of large (shown in red) and small chromosomes (green) in metaphase rosettes of human (**F**) and chicken (**G**) cells. In human cells (**F**), all chromosomes abut the tight bundle of microtubules of the mitotic spindle. The centromeres of all chromosomes form a ring in the equatorial plane of the spindle (compare with the prometaphase rosette on **E**). The gravity centres of small chromosomes are situated closer to the spindle axis than the gravity centres of large chromosomes. In chicken cells (**G**), the macrochromosomes surround the bundle of central microtubules, while the microchromosomes are predominantly located between the central microtubules of the spindle. (**H**) Scheme illustrating the hypothesis that the radial arrangement of chromosome territories in the cell nucleus has its origin in the chromosome arrangement in the preceding metaphase plate and is maintained to a great extent during the entire cell cycle. Metaphase as well as anaphase rosettes of flat, adherently growing cells (upper row) are typically perpendicular to the substratum. During telophase, the separated rosettes decline until they are parallel to the substratum. The formation of a spherical nucleus (lower row) requires an expansion of the decondensing chromatin along the spindle axis.

Consequently, centromeres of all human chromosomes form a ring in the equatorial plane of the spindle (Figure 5E, F), while the gravity centres of small chromosomes are situated closer to the spindle axis than the gravity centres of large chromosomes (Figure 5F). The radial chromosome arrangement in the mitotic cells may be reinforced by the spindle and provide the starting point for the radial arrangements of chromosome territories in the reforming daughter cell nuclei (see Figure 5H). Metaphase as well as anaphase rosettes of flat cells adherently growing *in vitro* are typically perpendicular to the substratum (e.g. a coverslip, Figure 5E, H upper row). After separation of chromatids, the two anaphase rosettes move to the opposite spindle poles. During telophase, the two sister rosettes decline until they are parallel to the substratum (Figure 5E, H upper row) and chromosomes start to decondense. The formation of a spherical nucleus (Figure 5H lower row) requires an expansion of the decondensing chromatin along the spindle axis. While side-by-side arrangements of chromosomes may change when a cell enters mitosis and forms the metaphase plate, the side-by-side arrangements established during telophase–early G1 are probably maintained to a large extent during the entire interphase (Boveri 1909 and our own unpublished observations).

In humans, the radial position of some chromosome territories cannot be explained by the action of the spindle. For example, in human lymphocyte nuclei, chromosome territories #18, 19 and Y show distinctly different positions: #18 and Y are located at the nuclear periphery and #19 in the nuclear centre (Croft *et al.* 1999, Cremer *et al.* 2001). This distribution does not fit a simple correlation of chromosome DNA content and radial CT positioning and further emphasizes a need for specific interactions between chromatin and other nuclear structures (lamina etc.) in order to establish higher-order chromatin arrangements.

Correlation of higher-order chromatin arrangements with replication timing and gene density

Our data confirm previous observations (Schmid *et al.* 1989, Ponce de Leon *et al.* 1992, McQueen et al. 1998) that microchromosomes are predominantly early replicating with a small proportion of late-replicating segments. These late replicating segments may partly coincide with the heterochromatin blocks visualized by C-banding (Schmid *et al.* 1989). The preferential position of mid–late replicating chromatin at the nuclear periphery and the central position of early replicating chromatin previously observed in mammalian cell nuclei (Ferreira *et al.* 1997, Sadoni *et al.* 1999) was confirmed for chicken cells by double replication labelling experiments. In humans, the majority of smaller autosomes are early replicating. In comparison to the later replicating larger chromosomes, they have a higher average content of CpG islands (Craig & Bickmore 1994) and a higher gene density as predicted by the estimation of ESTs (Deloukas *et al.* 1998). A specific radial chromatin arrangement with regards to the preferential positioning of relatively gene-dense early replicating chromatin in the nuclear interior and late replicating relatively gene-poor chromatin at the nuclear periphery, seems to be an evolutionary conserved motif for the organization of the nucleus in both chicken and human cells. It should be noted that we did not detect in chicken cell nuclei a rim of mid–late replicating chromatin around the nucleoli while such a rim is typically observed around nucleoli in human cells (O'Keefe *et al*. 1992, Sadoni *et al*. 1999). This difference may reflect the fact that the chicken genome bears much less heterochromatin than the human genome.

Future comparative studies could help to gain more insight into evolutionary conserved cell cycle and cell type specific motifs of higher-order chromatin arrangements. The chromosome-specific paint probes generated from *Gallus gallus domesticus* can identify orthologous chromosomes of other bird species with distinctly different karyotypes. Thus, chicken chromosome paint probes or painting pools could be used to identify the distribution pattern of orthologous genomic segments in nuclei of different bird species. Species with highly divergent karyotypes offer a way to analyse the contribution of chromosome size, gene density and replication timing as key factors for a conserved radial arrangement of chromatin.

Acknowledgements

Paint probes for chicken chromosomes were developed in the laboratory of Dr M. Ferguson-Smith (University of Cambridge, UK). We thank Dr. W.C. Earnshaw (University of Edinburgh, UK) for providing antibodies against CENP-C. We are grateful to Dr. J.-M. Buerstedde (University of Hamburg, Germany) for the generous gift of DT-40 cells. This work was supported by grants from the Deutsche Forschungsgemeinschaft to T. Cremer (Cr 59/20-1), from the European Community to C. Cremer (FIGH-CT1999-00011) and to J. Wienberg (BIO4-CT98-0228, AVIANOME), from the Bundesministerium für Bildung und Forschung to J. Wienberg (DLR01 KW 96142). G.K. received a grant from the Deutsche Forschungsgemeinschaft for graduates "modelling and scientific computing".

References

Bajer AS, Molé-Bajer J. (1972) Spindle dynamics and chromosome movements. In: Bourne GH, Danielli JF, eds. *International Review of Cytology*. New York & London: Academic Press.

Boveri T (1909) Die Blastomerehkerne von Ascaris megalocephala und die Theorie der Chromosomenindividualität. *Arch Zellforsch* **3**: 181–268.

Burt DW, Bruley C, Dunn IC *et al.* (1999) The dynamics of chromosome evolution in birds and mammals. *Nature* **402**: 411–413.

Chaly N, Brown DL (1988) The prometaphase configuration and chromosome order in early mitosis. *J Cell Sci* **91**: 325–335.

Craig JM, Bickmore WA (1994) The distribution of CpG islands in mammalian chromosomes [see comments]. [Published erratum appears in *Nat Genet* 1994 Aug;7(4): 551.] *Nat Genet* **7**: 376–382.

Cremer T, Cremer C (2001) Chromosome territories, nuclear architecture and gene regulation in mammalian cells. *Nat Rev Genet* **2**: 292–301.

Cremer T, Kreth G, Koester H *et al.* (2000) Chromosome territories, interchromatin domain compartment, and nuclear matrix: an integrated view of the functional nuclear architecture. *Crit Rev Eukaryotic Gene Expression* **12**: 179–212.

Cremer M, v. Hase J, Volm T *et al.* (2001) Non-random radial higher-order chromatin arrangements in nuclei of diploid human cells. *Chromosome Res* **9**: 541–567.

Croft JA, Bridger JM, Boyle S, Perry P, Teague P, Bickmore WA (1999) Differences in the localization and morphology of chromosomes in the human nucleus. *J Cell Biol* **145**: 1119–1131.

Deloukas P, Schuler GD, Gyapay G *et al.* (1998) A physical map of 30,000 human genes. *Science* **282**: 744–746.

Dietzel S, Weilandt E, Eils R, Münkel C, Cremer C, Cremer T (1995) Three-dimensional distribution of centromeric or paracentromeric heterochromatin of chromosomes 1, 7, 15 and 17 in human lymphocyte nuclei studied with light microscopic axial tomography. *Bioimaging* **3**: 121–133.

Emmerich P, Loos P, Jauch A *et al.* (1989) Double in situ hybridization in combination with digital image analysis: a new approach to study interphase chromosome topography. *Exp Cell Res* **181**: 126–140.

Ferreira J, Paolella G, Ramos C, Lamond AI (1997) Spatial organization of large-scale chromatin domains in the nucleus: a magnified view of single chromosome territories. *J Cell Biol* **139**: 1597–1610.

Griffin DK, Habermann F, Masabanda J *et al.* (1999) Micro- and macrochromosome paints generated by flow cytometry and microdissection: tools for mapping the chicken genome. *Cytogenet Cell Genet* **87**: 278–281.

Hedges SB, Parker PH, Sibley CG, Kumar S (1996) Continental break-up and the ordinal diversification of birds and mammals. *Nature* **381**: 226–229.

Kreth G, Edelmann P, Münkel C, Langowski J, Cremer C (2001) Translocation frequencies for X and Y chromosomes predicted by computer simulations of nuclear structure. *Chromosome Structure Function* (in press).

Lander ES, Linton LM, Birren B *et al.* (2001) Initial sequencing and analysis of the human genome. International Human Genome Sequencing Consortium. *Nature* **409**: 860–921.

Leonhardt H, Rahn HP, Weinzierl P *et al.* (2000) Dynamics of DNA replication factories in living cells. *J Cell Biol* **149**: 271–280.

Lesko SA, Callahan DE, LaVilla ME, Wang ZP, Ts'o PO (1995) The experimental homologous and heterologous separation distance histograms for the centromeres of chromosomes 7, 11, and 17 in interphase human T-lymphocytes. *Exp Cell Res* **219**: 499–506.

Macgregor H, Varley J (1988) *Working with Animal Chromosomes.* 2nd edn. John Wiley & Sons.

McQueen HA, Fantes J, Cross SH, Clark VH, Archibald AL, Bird AP (1996) CpG islands of chicken are concentrated on microchromosomes. *Nat Genet* **12**: 321–324.

McQueen HA, Siriaco G, Bird AP (1998) Chicken microchromosomes are hyperacetylated, early replicating, and gene rich. *Genome Res* **8**: 621–630.

Nagele R, Freeman T, McMorrow L, Lee HY (1995) Precise spatial positioning of chromosomes during prometaphase: evidence for chromosomal order. *Science* **270**: 1831–1835.

O'Brien SJ, Menotti-Raymond M, Murphy WJ *et al.* (1999) The promise of comparative genomics in mammals. *Science* **286**: 458–462, 479–481.

O'Keefe RT, Henderson SC, Spector DL (1992) Dynamic organization of DNA replication in mammalian cell nuclei: spatially and temporally defined replication of chromosome-specific alpha-satellite DNA sequences. *J Cell Biol* **116**: 1095–1110.

Östergren G (1945) Transverse equilibria on the spindle. *Bot Nat* **4**: 467–468.

Pettmann B, Louis JC, Sensenbrenner M (1979) Morphological and biochemical maturation of neurones cultured in the absence of glial cells. *Nature* **281**: 378–380.

Pichugin AM, Galkina SA, Potekhin AA, Punina EO, Rautian MS, Rodionov AV (2001) The detection of the size of a smallest chicken (Gallus gallus domesticus) microchromosome by pulsed-field gel electrophoresis (PFGE). *Genetika (Russ.)* **37**: 1–4.

Ponce de Leon FA, Li Y, Weng Z (1992) Early and late replicative chromosomal banding patterns of Gallus domesticus. *J Hered* **83**: 36–42.

Popp S, Scholl HP, Loos P *et al.* (1990) Distribution of chromosome 18 and X centric heterochromatin in the interphase nucleus of cultured human cells. *Exp Cell Res* **189**: 1–12.

Primmer CR, Raudsepp T, Chowdhary BP, Moller AP, Ellegren H (1997) Low frequency of microsatellites in the avian genome. *Genome Res* **7**: 471–482.

Pyrpasopoulou A, Meier J, Maison C, Simos G, Georgatos SD (1996) The lamin B receptor (LBR) provides essential chromatin docking sites at the nuclear envelope. *Embo J* **15**: 7108–7119.

Rice JC, Allis CD (2001) Histone methylation versus histone acetylation: new insights into epigenetic regulation. *Curr Opin Cell Biol* **13**: 263–273.

Rieder CL, Salmon ED (1994) Motile kinetochores and polar ejection forces dictate chromosome position on the vertebrate mitotic spindle. *J Cell Biol* **124**: 223–233.

Sadoni N, Langer S, Fauth C *et al.* (1999) Nuclear organization of mammalian genomes. Polar chromosome territories build up functionally distinct higher order compartments. *J Cell Biol* **146**: 1211–1226.

Sadoni N, Sullivan KF, Weinzierl P, Stelzer EH, Zink D (2001) Large-scale chromatin fibers of living cells display a discontinuous functional organization. *Chromosoma* **110**: 39–51.

Schermelleh L, Solovei I, Zink D, Cremer T (2001) Two-colour fluorescence labelling of early and mid-to-late replicating chromatin in living cells. *Chromosome Res* **9**: 77–80.

Schmid M, Enderle E, Schindler D, Schempp W (1989) Chromosome banding and DNA replication patterns in bird karyotypes. *Cytogenet Cell Genet* **52**: 139–146.

Smith J, Burt DW (1998) Parameters of the chicken genome (Gallus gallus). *Anim Genet* **29**: 290–294.

Smith J, Bruley CK, Paton IR *et al.* (2000) Differences in gene density on chicken macrochromosomes and microchromosomes. *Anim Genet* **31**: 96–103.

Solovei I, Walter J, Cremer M, Habermann F, Schermelleh L, Cremer T (2001) FISH on three-dimensionally preserved nuclei. In: Squire J, Beatty B, Mai S, eds. *FISH: A Practical Approach*. Oxford: Oxford University Press.

Sun HB, Yokota H (1999) Correlated positioning of homologous chromosomes in daughter fibroblast cells. *Chromosome Res* **7**: 603–610.

Sun HB, Shen J, Yokota H (2000) Size-dependent positioning of human chromosomes in interphase nuclei. *Biophys J* **79**: 184–190.

Telenius H, Pelmear AH, Tunnacliffe A *et al.* (1992) Cytogenetic analysis by chromosome painting using DOP-PCR amplified flow-sorted chromosomes. *Genes Chromosomes Cancer* **4**: 257–263.

Wade PA (2001) Methyl CpG binding proteins: coupling chromatin architecture to gene regulation. *Oncogene* **20**: 3166–3173.

White MJ (1961) The chromosomes. In: *Methuen Monographs on Biological Subjects*. London: Methuen & Co. Ltd.

Zink D, Cremer T, Saffrich R *et al.* (1998) Structure and dynamics of human interphase chromosome territories in vivo. *Hum Genet* **102**: 241–251.